Catalysis Today 138 (2008) 84–96

Contents lists available at ScienceDirect

Catalysis Today

journal homepage: www.elsevier.com/locate/cattod

Model catalysis by metals and alloys: From single-crystal surfaces to well-defined nano-particles

Jean-Claude Bertolini *

Institut de Recherches sur la Catalyse et l'Environnement de LYON IRCELYON, UMR 5256 CNRS-UCBLyon1, 2 avenue Albert Einstein, F-69626 Villeurbanne cedex France

ARTICLE INFO

Article history:
Available online 24 June 2008

Keywords:
Model catalysis
Metals and alloys
Surface science

ABSTRACT

During the last decades surface science has played an important role for modelling surface chemistry on metallic surfaces and understanding catalytic processes for simple reactions. Progresses are now made possible by the recent development of specific tools for characterising at the nanoscale level model materials and following the kinetics of reactions on these materials of small area in dedicated reactors.

It needs the preparation, and characterisation at the atomic level, of well-defined materials. They can be either single-crystal surfaces having a well-defined orientation or in shape of model supported nano-particles. Most has been done in the framework of monometallic materials, but more difficult is the preparation of well-defined alloy surfaces and surface alloys, and the elaboration of alloy nano-particles well-defined in size and composition.

Kinetic studies in dedicated reactors show how the catalytic behaviour of model samples may depend on the specific sites present at surface. For example, surface sites having a low coordination number (like steps, kinks, edges and corners) are very efficient for bond-breaking. In bi-metallics, ad-layers of a given metal on a foreign substrate may show new and original structures having very specific catalytic properties. Thus, works on catalysis at the atomic scale proposes new active/selective sites, and it is now a challenge to design new industrial catalysts on the basis of these fundamental works.

In order to move near the conditions for real catalysis one has now to bridge the "pressure gap", i.e. to make in situ (during reaction under pressure of reactants) characterisation of both the surface itself and ad-species. This needs the development of specifics tools able to work in such conditions. This is a challenge for today and future works in the field of model catalysis.

1. Introduction

Most of the chemical processes (more than 80%) imply at least one step of catalysis. Heterogeneous catalysis is a priori more promising than homogeneous catalysis since it is easier to recover solid catalysts after reaction, which allows to less costly, and then more friendly, processes. Moreover, it is necessary to get very active catalysts reaching 100% selectivity, in order to make on one side economy of (often rare and expensive) materials and, on the other side, to avoid waste and undesired products. Industrial catalysts are very complex since they have different active sites exposed, and it is somewhat difficult to draw safe conclusion on the elementary steps of the catalytic process and on the most efficient surface sites. These points are key tasks for the present and future in catalysis. The so-called "surface science" approach offers a way to progress in this field. It needs the use of well-defined materials together with the use of specific tools for surface characterisation at the atomic/molecular level, i.e. at the sub-nanometric scale. Over the past 40 years research works have been devoted to the surface science approach of catalysis, following the pioneer works of Gabor Somorjaï and Gerhard Ertl (chemistry Nobel laureate in 2007). The surface science studies have been made possible with the development of ultra high vacuum (UHV), i.e. nearby 10^{-10} torr, and of high-performance tools for the characterisation of their surface atomic and electronic structure, allowing the possible preparation of surfaces and their observation in a delay of time without significant contamination. Indeed, one has to keep in mind that under 10^{-6} torr of reactive gas the surface is covered by one monolayer (ML) in 1 s, if the sticking probability is unity; this is actually the case for highly active metallic surfaces with respect to many reactants.

The role of catalyst surface structure in controlling reaction rates and reaction selectivity has been first demonstrated with the use of well oriented single-crystal surfaces. In order to bridge the so-called "materials gap" researches have more recently been devoted to the elaboration and characterisation at the atomic level

* Tel.: +33 4 72 44 53 09; fax: +33 4 72 44 53 99.
E-mail address: jean-claude.bertolini@ircelyon.univ-lyon1.fr.

0920-5861/$ – see front matter © 2008 Elsevier B.V. All rights reserved.
doi:10.1016/j.cattod.2008.04.039

of well-defined nano-particles deposited on flat and well-defined supports.

The first parts of the present paper would like to address the ways to get monometallic materials in shape of both single-crystals and small particles exhibiting different surface sites; their specific reactivity will be illustrated with considering some catalytic reactions.

Bi-metallic alloy surfaces and surface alloys will be also considered, with a view focused on the possible surface segregation of one element at surface, depending on their thermodynamic properties.

Most of the earlier works in this field have been made under very low pressure; this is actually due to intrinsic limitations of the diffraction and spectroscopic techniques used, mainly based on the impact and/or emission of low energy electrons and/or ions. In order to move near the conditions for real catalysis one has now to bridge the "pressure gap", i.e. to make in situ (during reaction under pressure of reactants) characterisation of both the surface itself and ad-species. This needs the development of specifics tools able to work in such conditions, a challenge for future works in the field of model catalysis. The last part of this paper would like to address this point.

2. Model catalysts

2.1. Single-crystal surfaces with well-defined orientation

It is a long way to get single-crystal surfaces having a well-defined orientation, with as less defects as possible.

This needs at first a single-crystal growth (generally by Czochralski or Bridgman method for transition and noble metals) in shape of a single-crystal bar with using materials of high purity (>99.99%). In a second step, the single-crystal bar has to be cut near the desired orientation obtained from X-ray Laue patterns. This has to be done without important in-depth destructuration of the single-crystal, which is actually achieved by electro-erosion. At last, a precise orientation and flatness of the surface is obtained by X-ray goniometry followed by mechanical or chemical polishings along the desired face. The orientation accuracy so obtained is typically +/−0.1°.

Moreover, one has to notice that further treatments (heatings, Ar^+ ion bombardments, oxidation and reduction, etc.) have to be done under UHV conditions to achieve the surface preparation.

On the resulting surfaces the outer atoms are at a different coordination than the atoms in the bulk. This is a priori a non-stable situation which allows to changes in the interatomic distances with respect to the well known parameters in the bulk crystals. Actually, there is an upward relaxation of the overlayer distance on clean surfaces; the amplitude of this relaxation, measured by low energy electron diffraction (LEED), is more important for surfaces exhibiting less coordinated surface atoms [1]. For nickel, a face centred cubic (fcc) crystal (coordination number of bulk atoms = 12), the downward relaxation of the close-packed (1 1 1) surface (coordination number of surface atoms = 9) is only nearby 2%, while the first interlayer spacing is contracted by around 8–9% on the "more open" (1 1 0) face (coordination number of surface atoms = 7) [2]. The relaxation is in fact rapidly damped but it can extend to three interlayer spacings [1]. For example, on Ni(1 1 0) the second interspacing has been found to be expanded by 3% [2]. This oscillatory relaxation of the interlayer spacing found on the Ni(1 1 0) surface is very similar to what has been reported for Al(1 1 0) and Cu(1 1 0) and confirms this general trend for fcc (1 1 0) faces.

Moreover, reconstructions can occur in the outer layers, with lateral and vertical displacements of surface atoms. This is effective for some metals like Ir(1 1 0), Pt(1 0 0), Pt(1 1 0), Au(1 1 1) and Au(1 1 0).

A schematic representation of unreconstructed dense faces of fcc crystals is given for illustration in Fig. 1.

Surfaces having high-index Miller indices exhibit specific surface sites, like steps and kinks (Fig. 2). They are produced by cutting crystals slightly away from their dense crystallographic orientation. They are in shape of more or less large terraces generally separated by steps of monoatomic height on metals. In the often used notation proposed by Lang et al. [3], a [7(1 1 1) × (1 0 0)] surface is constituted by (1 1 1) oriented terraces having a width of seven atomic rows with steps having a (1 0 0) orientation. Such a surface can be also named following its Miller indices: (7 5 5). It is a way to produce model catalysts exhibiting a collection of specific site defects with low coordina-

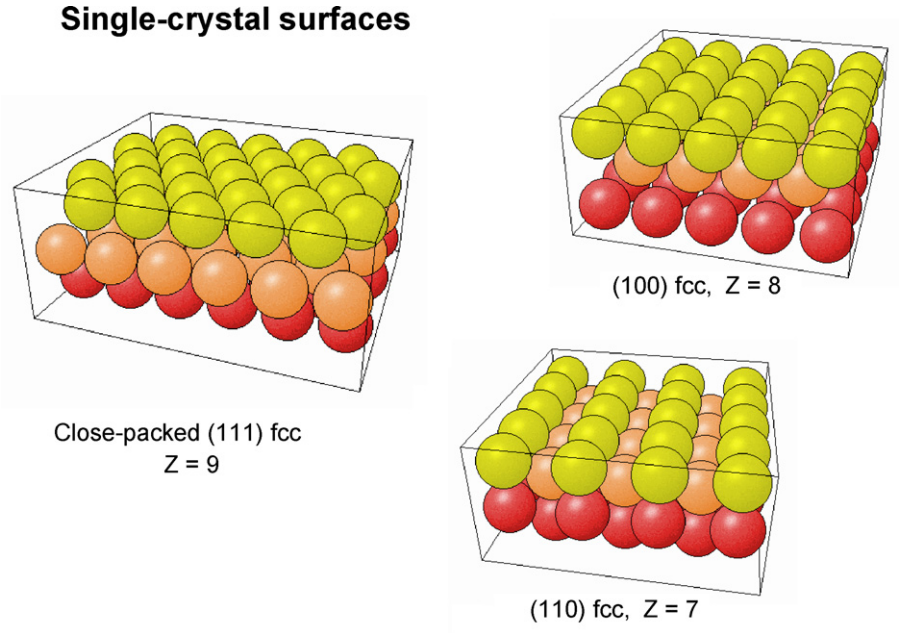

Fig. 1. Schematic representation of unreconstructed dense faces of fcc crystals.

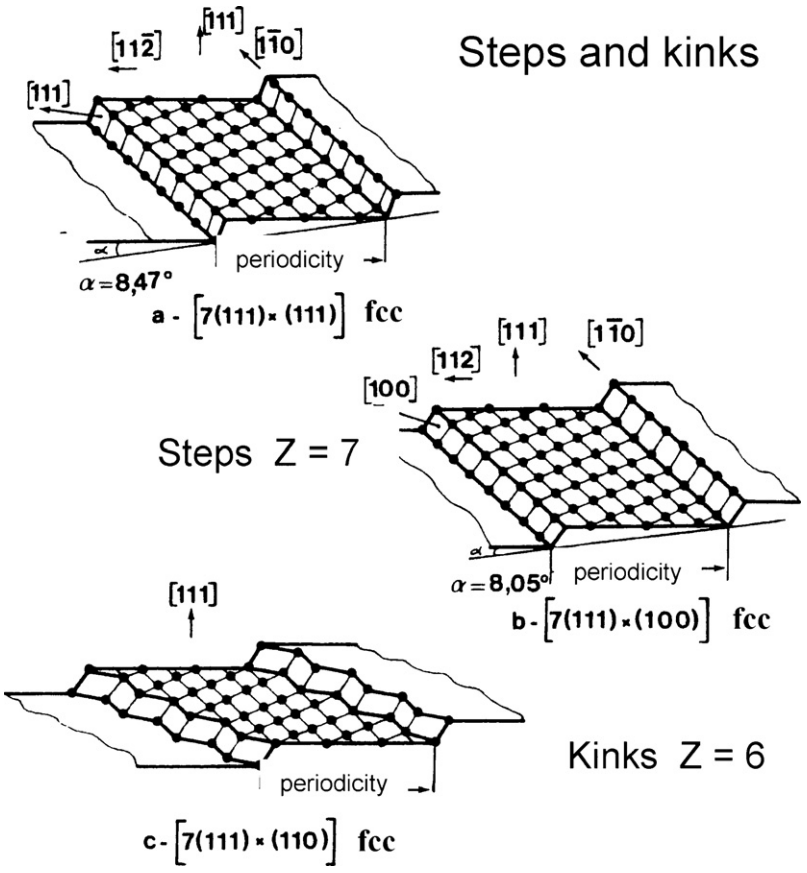

Fig. 2. Schematic representations of some fcc single-crystal surfaces with a variety of surface structures showing step and kink defects.

tion and a given geometry. For example, the [7(1 1 1) × (1 1 0)] kinked surfaces of fcc crystals exhibit surface atoms with an unusual coordination number as low as 6.

We will see further that the catalytic properties of single-crystal surfaces may depend strongly on their surface structure and composition.

2.2. Model supported clusters

The properties of nano-particles, including chemical reactivity, exhibit a marked dependency on their size, shape (and composition for alloys). For a good understanding, it is therefore necessary to prepare nano-particles having a narrow size (and composition) distribution, and to characterise their shape and exposed facets at the atomic level. In order to do so, works are performed on catalytic samples in shape of nano-particles deposited on flat and well-defined oxide supports [4–6]. It is a way to simulate the situation found in real catalysts.

Vapour deposition of metals (or, but at a less extent, deposition of pre-formed clusters) under UHV conditions on previously prepared supports is the way generally used to get model nano-particles. The resulting sample will depend on the preparation of the substrate, on the metal coverage and on the temperature at which the deposition and/or further thermal treatments will be made.

We will examine here only the preparation of two single-crystal oxide surfaces (magnesium oxide [4,7] and aluminium oxide [6]) used as supports of Pd clusters.

Resulting samples depend upon the preparation of the MgO(1 0 0) support. Pd clusters obtained by vapour deposition at room temperature on a MgO(1 0 0) support cleaved under UHV are rather large and located along the steps in the (1 0 0) directions; alignments are separated by flat terraces of a mean width of 250 nm (Fig. 3a). On the contrary, the same MgO surface cleaved in air and in situ cleaned no longer shows step decoration by metal clusters (Fig. 3b); the density of nuclei is then largely increased and the Pd particle size is largely smaller for the same metal coverage.

Ultra-thin oxide films grown on a metallic substrate can be a way to circumvent problems with the insulating nature of bulk oxides, and apply many surface science techniques to characterise them. Freund et al. have demonstrated that cycles of oxidation at 500–550 K, and subsequent annealing to 1000–1100 K, of a NiAl(1 1 0) single-crystal allows the formation of a very thin and well-structured aluminium oxide film [6,8]. Scanning tunnelling microscopy (STM) measurements and density-functional theory calculations have shown that the surface is oxygen deficient and thus processes favourable adsorption sites [8]. The model catalysts prepared by atomic beam deposition on this oxide support depend upon the temperature and the amount of Pd deposited (Fig. 4b and c); the particles have a relatively uniform, but variable, size depending on the amount of Pd deposited. On a hydroxylated support the particles are considerably smaller and distributed across the entire surface (Fig. 4d); one can so obtain high concentration of small particles at room temperature. In the same way, it has been shown that a mild oxidation of a clean Ni_3Al(1 1 1) substrate leads to the formation of a very thin alumina film (~0.5 nm) having a well ordered commensurable atomic lattice (Fig. 5) [9]. A network of defects having a large hexagonal lattice (4.14 nm) is formed which can serve as template for preferential adsorption of metal clusters [10].

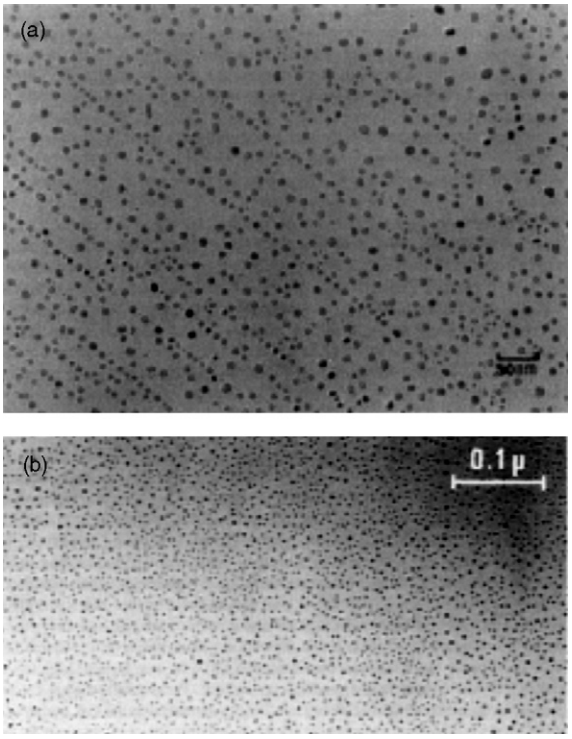

Fig. 3. Pd clusters deposited on MgO(1 0 0) after (a) UHV cleavage and (b) air cleavage and in situ cleaning of the MgO support [from ref. [4]].

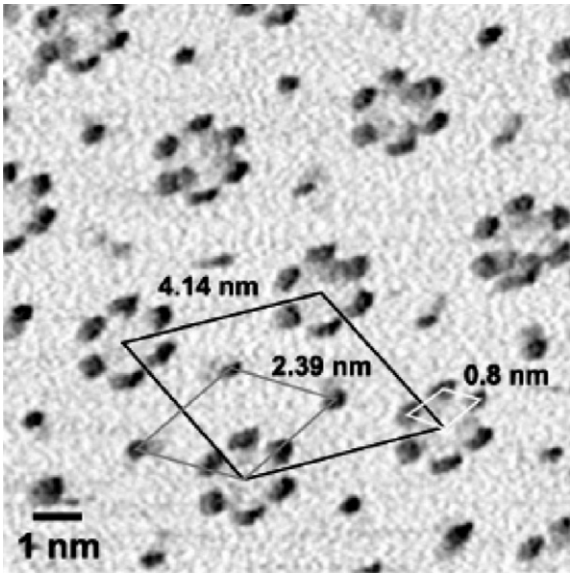

Fig. 5. STM image of the nanostructurated thin alumina film obtained by mild oxidation of a $Ni_3Al(1\ 1\ 1)$ single-crystal [from ref. [9]].

2.3. Surface alloys and alloy surfaces

Bi-metallic surface alloys can be obtained by deposition of controlled overlayers of a foreign metal on a metallic substrate.

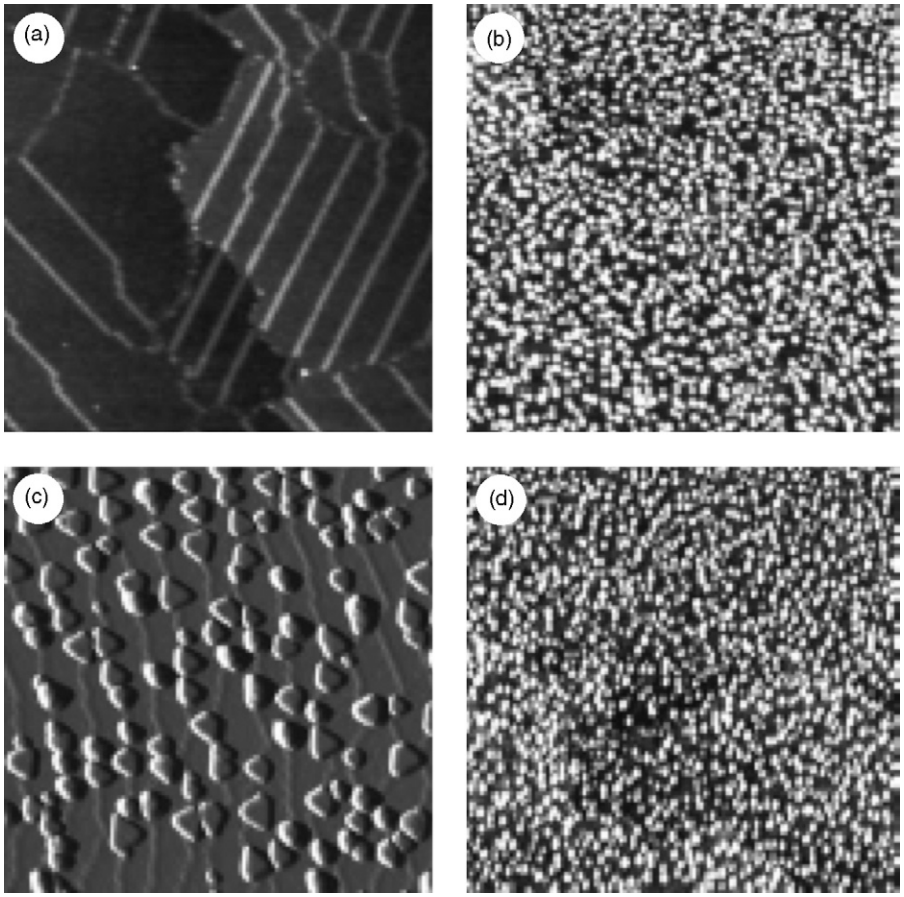

Fig. 4. STM images (100 nm × 100 nm) of: (a) clean alumina film on NiAl(1 1 0), (b) 0.02 nm Pd deposited at 90 K, (c) 0.2 nm Pd deposited at 300 K and (d) 0.02 nm Pd deposited on a prehydroxylated film at 300 K [from ref. [6]].

This leads to well-defined samples when using single-crystals as substrates [11].

The surface composition of bi-metallic alloys can be strongly different of the nominal bulk composition. Indeed, a strong segregation of one component towards the surface outer layer can exist, which depend on [12,13]:

(i) the difference of surface energy of the two components; the system tends to minimize its free energy by pushing at the surface the element of lower surface tension,
(ii) the elastic strain relaxation, which tends to expel the minority element mainly when it is the bigger one,
(iii) the mixing enthalpy, which tends to amplify the influence of the two previously mentioned effects when it is positive, or on the contrary tends to moderate this effect if it is negative. In such a case, the layer by layer composition has a tendency to oscillate.

In Fig. 6 are reported the expected values of Pd surface composition as a function of the nominal bulk composition for (1 1 1) faces of Pd–X (X = Ni, Pt, Cu, Ag and Au) alloys [13]. One can see that the surface composition can be largely different from that of the nominal bulk composition; for example, the Pd content at the very surface of PdPt and PdNi alloys is expected to be very important even if the bulk content is only a few %. This has been actually verified experimentally with using low energy ions scattering spectroscopy (LEIS), a technique able to check the composition of the outer layer [13–15]. Moreover, this surface enrichment is more pronounced on more open surfaces [13].

In bi-metallic alloys, strains do exist at the surface when there is a large surface segregation of one component and a big difference of the atomic radii of the two components; the stress is generally relaxed via surface reconstructions, generating new and original structures. It is for example the case for the Pd_8Ni_{92}(1 1 0) surface, showing a surface Pd content as large as 81% and a large difference of atomic radii (Pd is nearby 9% bigger tan Ni), as evidenced by STM and/or grazing X-ray diffraction (XRD) techniques [16,17] (Fig. 7). A ($N \times 1$) superstructure (with N = 5–6) is formed in the surface region with alignments separated by about 1 nm parallel to the [0 0 1] direction (left part of Fig. 7); strains are actually relaxed by in- and out-of plane displacements of some surface atoms every N substrate atoms along the [1 1 0] rows (right part of Fig. 7).

Tentative preparation of model bi-metallic nano-particles can be made by simultaneous co-evaporation of two metals on a well-defined oxide support. But, in such a "one step" process the composition changes with the particle size because the condensation coefficients are normally not the same for the two components. If the two metals are deposited successively ("two step" process) monometallic and bi-metallic particles are generally obtained. However, it has been shown that the second metal can be deposited uniformly on a first metal trapped on all the defects [18].

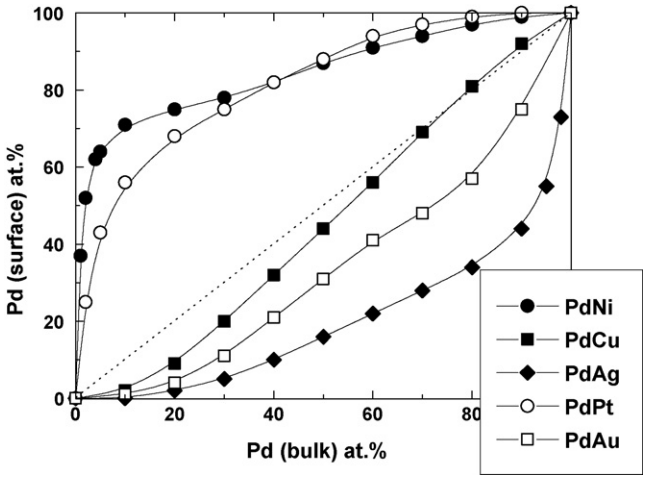

Fig. 6. Predicted values for the composition of the first atomic layers of (1 1 1) Pd–X alloys (X = Ni, Pt, Cu, Ag and Au) [from ref. [13]].

To overcome this difficulty, the laser vaporisation of bulk alloys (Fig. 8a) offers a unique way to obtain bi-metallic nano-particles having a narrow size distribution and a homogeneous composition, as shown for two Pd–Pt alloys having a mean size of nearby 3 nm (Fig. 8b) [19,20]. As for bulk Pd–Pt alloys, the first outer layer of small particles (measured by LEIS) is largely enriched into Pd [19,21].

2.4. Experimental set-up

Surfaces used as model catalysts, for which structure, composition and oxidation state could be measured on the atomic scale by many surface science tools, are therefore in the form of small area ($\sim$1 cm^2) single-crystals or very thin films. They exhibit only very few surface sites ($\sim 10^{15}$ surface atoms) when compared to real catalysts deposited on large surface area supports (typically $>$100 m^2/g). This needs the development of very specific tools with specially designed reactors.

Fig. 9 shows a scheme of a typical set of instrument developed to prepare model catalytic surfaces and characterise them under UHV conditions, with transfer of samples to operate at high reaction pressures in dedicated reactors for kinetic measurements.

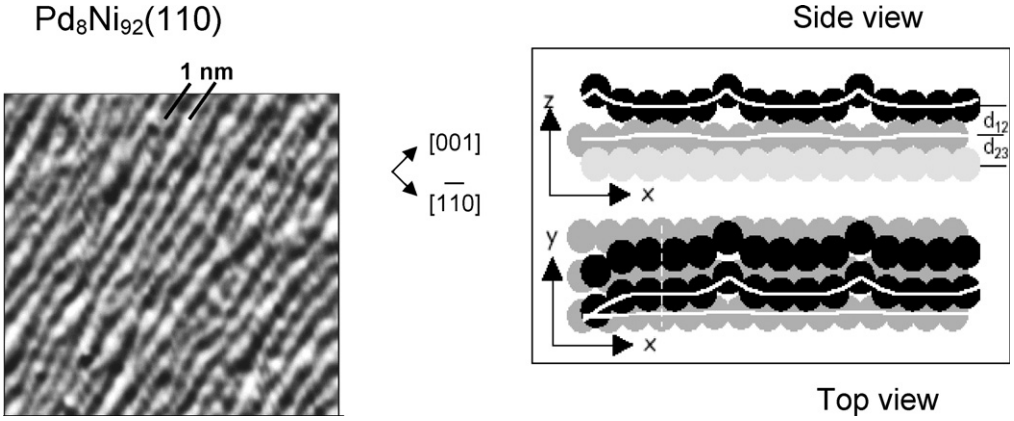

Fig. 7. Left: STM image of the Pd_8Ni_{92}(1 1 0) [from ref. [16]], right: side and top views of the structure of the clean Pd_8Ni_{92}(1 1 0) surface deduced from grazing incidence X-ray diffraction [from ref. [17]].

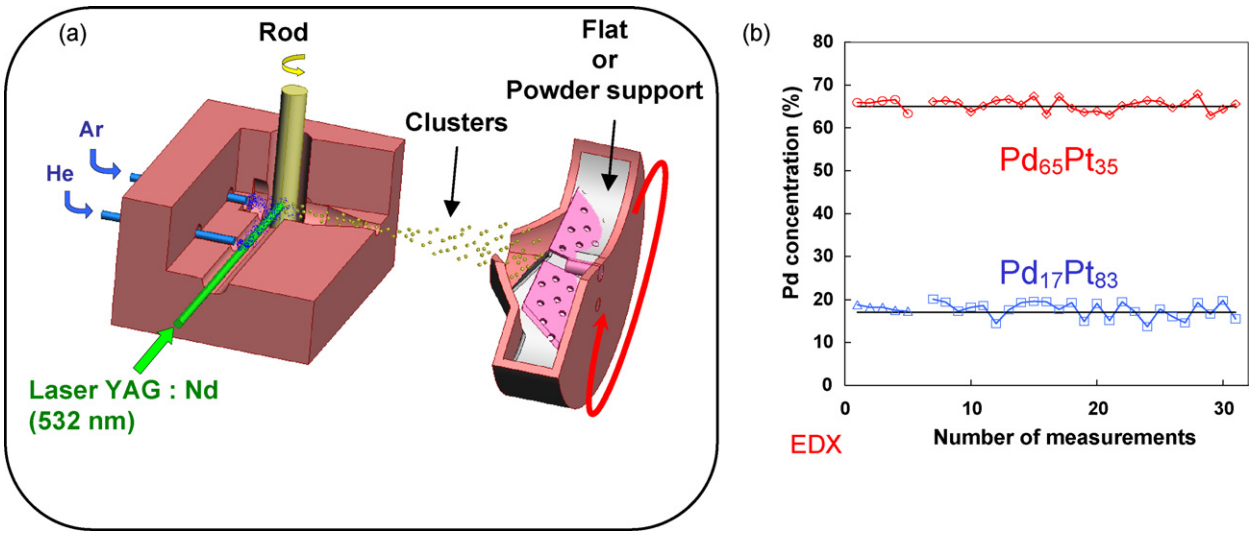

Fig. 8. (a) Schematic representation of the instrument for laser vaporisation to produce nano-particles from a bulk target [19]; (b) Pd concentration of a collection of supported $Pd_{17}Pt_{83}$ and $Pd_{65}Pt_{35}$ clusters obtained by laser vaporisation from bulk Pd–Pt alloys [20].

Moreover, "in situ" measurements need to design reactors allowing the possible use of specific techniques able to measure the surface structure and the ad-species of working model catalysts, like STM, grazing incidence XRD, sum frequency generation (SFG), polarisation-modulation infrared reflection absorption spectroscopy (PM-IRRAS), X-ray photoelectron spectroscopy (XPS), etc.

3. Catalysis on model surfaces

We will first consider the selective hydrogenation of 1,3-butadiene into butenes as an example of model studies of catalytic behaviour of mono- and bi-metallic model catalysts (Fig. 10). This is an important industrial reaction used for the elimination of butadiene (undesirable product for further polymerisation of alkenes) in C_4 cuts in petroleum chemistry, which occurs on transition metal catalysts such as Ni, Pd and Pt. Actually, Pd is the most efficient (active and selective) catalyst. The selectivity into butenes, defined by the ratio [butenes]/[butenes + butane], has to be as high as possible up to the complete conversion of butadiene. Indeed, one has to avoid the total hydrogenation into butane. It is controlled by two parameters. One is kinetic and measures the butene hydrogenation rate relative to the butene desorption rate. The other one is thermodynamic and depends on the relative adsorption coefficients of butadiene and butenes. This thermodynamic parameter turns out to be preponderant; it will fix the relative coverages in butadiene and butenes on the surface as a function of their relative partial pressure. A better selectivity will be observed if butadiene is largely more strongly adsorbed than butene.

This reaction has been studied on various single-crystal surfaces and model nano-particles.

3.1. 1,3-Butadiene hydrogenation on monometallic single-crystals and model nano-particles

As shown in Table 1, Pd is a most efficient (active and selective) catalyst than Ni and Pt. For the same surface orientation Pt is less active than Pd by at least one order of magnitude and its selectivity into butenes is only slightly more than 50%, even at low conversion. On the contrary, there is no butane formation on Pd even at high conversion. This is also the case for Pd and Pt particles supported

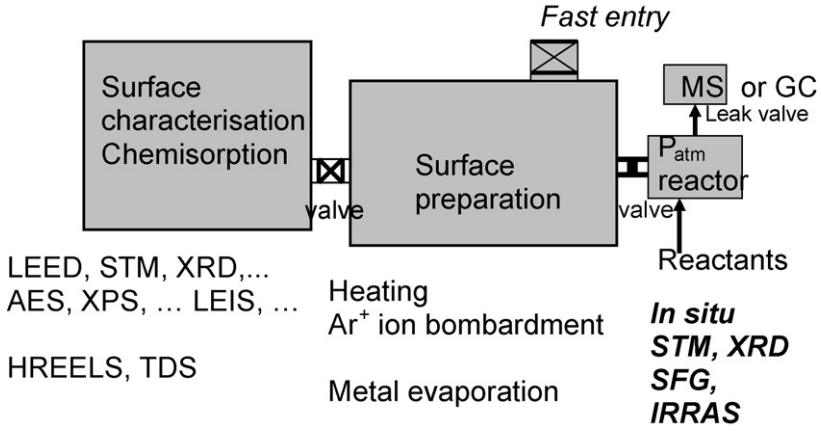

Fig. 9. Scheme of a typical system combining UHV cells for preparation and characterisation of model surfaces, and atmospheric pressure cell for catalytic and "in situ" (under pressure of reactants) measurements. LEED: low energy electron diffraction; STM: scanning tunnelling microscopy; XRD: X-ray diffraction; AES: Auger electron spectroscopy; XPS: X-ray photoelectron spectroscopy; LEIS (or ISS): low energy ion scattering (or ion scattering spectroscopy); HREELS: high resolution (vibration) electron energy loss spectroscopy; TDS: thermal desorption spectroscopy; SFG: sum frequency generation; IRRAS: infrared reflexion absorption spectroscopy.

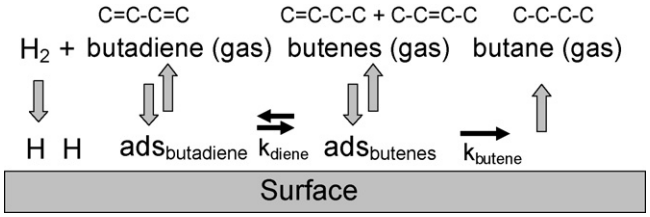

Fig. 10. The 1,3-butadiene hydrogenation reaction.

Table 1
Catalytic activity (butadiene to butenes) on various single-crystal faces of Ni, Pd and Pt (at 293 K, 10 torr H_2 and a hydrogen/butadiene ratio of 5–10)

	Pd(1 1 1)	Pd(1 1 0)	Pt(1 1 0)	Ni(1 1 0)
Catalytic activity ($\times 10^{15}$ mol cm^{-2} s^{-1})	0.42	2.15	0.1	0.2
Selectivity into butenes (%)	100%	100%	54%	100%

on SiO_2 [22]. Chemisorption studies of 1,3-butadiene at 300 K on Pt(1 1 1) and Pd(1 1 1), by X-ray absorption near edge spectroscopy (XANES) at the C-k_{edge}, argue in favour of the conservation of the π conjugation on Pd(1 1 1) indicating a di-π chemisorbed state; at the opposite, on Pt(1 1 1) the $C_{1s} \rightarrow \pi^*$ splitting is no longer observed, and the chemisorbed state is associated to a di-σ state [23]. It is experimentally difficult to characterise chemisorbed butene at 300 K since butene dehydrogenates in the absence of hydrogen, leading to the presence of adsorbed species similar to adsorbed butadiene on Pd(1 1 1) and to the formation of butylidyne like species on Pt(1 1 1). However, one can speculate that, under associative chemisorption conditions, butene (with a single C=C bond) is π adsorbed on Pd and di-σ adsorbed on Pt. Then, theoretical calculations show that the adsorption energy of (di-π adsorbed) butadiene is expected to be two times more than the adsorption energy of (π adsorbed) butene on Pd(1 1 1) (i.e. 36 kcal mol^{-1} vs. 17 kcal mol^{-1}), while they are the same for di-σ adsorbed butadiene and butene on Pt(1 1 1) (15 kcal mol^{-1}) [24]. This can explain the high selectivity of Pd as compared to Pt. Moreover, the large difference of activity between Pd and Pt can be the consequence of the two different adsorption states.

Hydrogenation reactions are generally considered as independent of the surface structure. But, results present in Table 1 show that the activity for the more open (1 1 0) face of Pd is largely higher than that of the close-packed (1 1 1) face. The lower activity of Pd(1 1 1) is probably due to the stronger binding of 1,3-butadiene to Pd(1 1 1) as compared to Pd(1 1 0) [25]. The activity difference can be thus either intrinsically the consequence of the modified state of activation for the chemisorbed molecule or indirectly due to a reduction of the surface hydrogen concentration when the hydrocarbon is more strongly adsorbed [26,27].

For such a reaction, the results of Freund and co-workers show how small Pd particles can act similarly to single-crystal surfaces [26–28]. At a first sight, their results (reported in Fig. 11) suggest that the kinetic behaviour is different for the three model catalysts although the product distribution follows a similar trend: smaller Pd particles seem a priori less active than larger ones. In fact, the turn over frequency (TOF) for butadiene hydrogenation calculated with using the number of surface Pd atoms in the (1 1 1) facets of particles is quite the same than for Pd(1 1 1) (insert of Fig. 11) and is clearly particle size independent. This suggests that the reaction takes place mainly on the (1 1 1) facets of Pd particles. Such a conclusion can only be drawn because they correlate the microscopic structural information on the Pd nano-particles (by

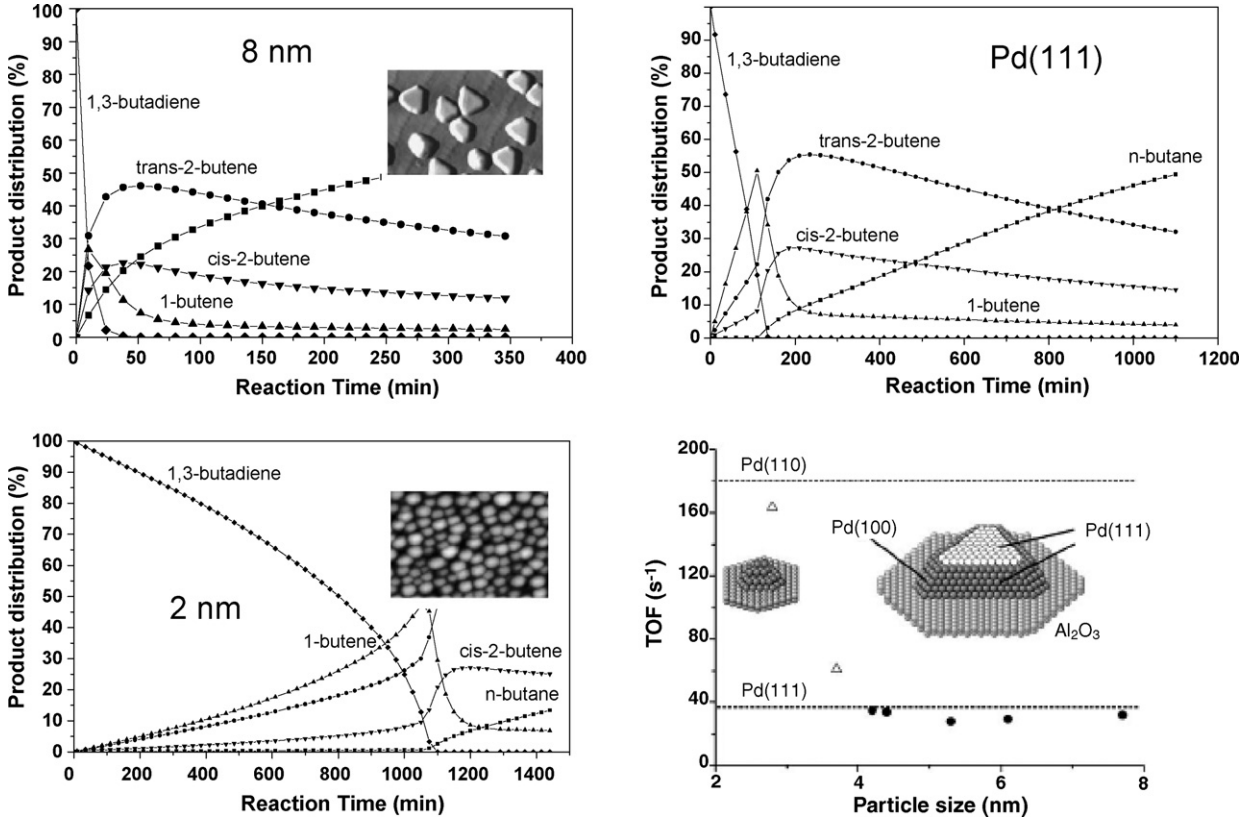

Fig. 11. Product distribution versus reaction time for 1,3-butadiene hydrogenation on model Pd nano-particles supported on Al_2O_3/NiAl (2 and 8 nm) and on a Pd(1 1 1) single-crystal (5 mbar 1,3-butadiene, 10 mbar H_2, 100 °C). In insert is given the turn over frequency (TOF) for the different catalysts [26,28].

STM) with their macroscopic catalytic properties. However, the behaviour of edge atoms remains unclear.

In any case, it is shown that the catalysts exhibit a constant activity at high butadiene pressure (i.e. low reaction time). Moreover, the reaction rate is limited by adsorption/desorption phenomena and not by a diffusion-control process, as indicated by the high apparent activation energy (75 kJ mol^{-1}).

As discussed previously, the results of Freund et al. agree with a catalytic activity for this reaction largely higher on the (1 1 0) than on the (1 1 1) oriented faces of palladium.

Summarising, surface science studies show that *butadiene hydrogenation* is *particle size independent* in spite of being *structure sensitive*. Actually, a palladium surface exhibiting the (1 1 0) orientation is more efficient for this reaction. But, (1 1 0) facets are not present on Pd particles in their equilibrium thermodynamic state, i.e. having a truncated cubo-octahedral shape with (1 1 1) facets (constituting the majority of the active surface) and with (1 0 0) side facets. It is now a challenge to prepare supported catalysts exhibiting a majority of (1 1 0) facets, for example with using epitaxy relation on well-structured supports able to have strong interaction with palladium.

3.2. Bi-metallic single-crystals

Chemisorbed CO has been widely used as a probe of the chemical properties of Ni, Pd and Pt dosed on many transition metals [29]. For one monolayer of Pd deposited on Ta, W, Mo, Re and Ru chemisorbed CO desorbs at considerably lower temperature than on pure Pd (Fig. 12). Correlations can be made between the binding energy shifts of the Pd_{3d} core level measured by XPS and the desorption temperature for chemisorbed CO: the higher is the shift upwards, the lower is the desorption temperature (Fig. 12). However, the reported chemical shifts (which reflect the electronic influence of the substrate) are underestimated by about 0.3–0.5 eV, since one has to take into account an additional surface versus bulk core level shift associated to the diminution of the coordination number of Pd surface atoms [30].

In conclusion, bi-metallic bonding can induce a significant redistribution of charge around the bonded metal (usually linked to the strength of the bi-metallic bond) which can determine the chemical reactivity of the system. However, we will see further that association of metals located on the same column of the periodic table (like Pd–Pt, Pd–Ni), which do not show significant chemical shift of their core level binding energy, can have largely different chemical reactivities.

Let us first consider the case of dilute alloys (Pd–Pt and Pd–Ni) for which very high surface segregation of Pd occurs.

For Pd_5Pt_{95} and Pd_5Ni_{95} polycrystalline alloys, the Pd surface content is quite the same but the catalytic performances with respect to the 1,3-butadiene hydrogenation reaction are very different (Table 2). Actually, for Pd_5Pt_{95} the catalytic properties can be seen as a simple superposition of the intrinsic properties of Pt and Pd outer atoms. Indeed, its activity (0.8×10^{15} mol cm^{-2} s^{-1}) ranges between that of pure Pd(1 1 1) (0.42×10^{15} mol cm^{-2} s^{-1}) and that of pure Pd(1 1 0) (2.15×10^{15} mol cm^{-2} s^{-1}), Pt being one order of magnitude less active than pure Pd. Very interesting is the noticeable increase of the activity observed for the Pd_5Ni_{95} (8×10^{15} mol cm^{-2} s^{-1}) even with respect to pure Pd. A different electronic influence of Pt and Ni surrounding atoms cannot be a priori invoked to explain the differences in catalytic activity of the two systems since Ni, Pd and Pt are located on the same column of the periodic table and have therefore similar electronic properties. Another explanation could be related to the difference of the strains undergone by the Pd surface atoms. Indeed, no stress is expected for Pd on top of a Pt rich alloy since Pd and Pt have near the same atomic radii. On the contrary, due to the large size misfit between Pd and Ni atoms (Pd has an atomic radius nearby 9% larger than Ni) the surface largely enriched into Pd will sustain a strong stress in PdNi alloys having a Ni rich matrix.

As shown in Fig. 7, the surface reconstruction evidenced by LEED, STM and grazing incidence X-ray diffraction on a Pd_8Ni_{92}(1 1 0) single-crystal is a way to relax, at least partially, the stress on a surface largely enriched into Pd. The catalytic activity of such a model catalyst is largely higher than that of pure Pd(1 1 0) (Table 3), and one may think that it is related to the new and original surface structure.

It has been also demonstrated that "surface alloys" obtained by Pd deposition on Ni(1 1 0) behave in the same way that "alloy surfaces" issued from Pd–Ni bi-metallic alloys having low nominal Pd bulk content, and showing a large Pd surface segregation [15,31,32].

Indeed, sub-monolayers of Pd deposited on Ni(1 1 0) are also largely more active than pure Pd (Table 3). As previously discussed, for sub-monolayers it is difficult to separate the possible electronic influence of the host metal (Ni) and the modifications due to the strain effects on the chemical properties of the deposit (Pd).

By the use of larger amounts of deposits one can hope to avoid the direct electronic influence of the substrate on the surface

Table 2
Concentration of the outer layer of clean Pd_5Pt_{95} and Pd_5Ni_{95}, and their catalytic activity and selectivity into butenes for the reaction butadiene → butenes (at 300 K, 10 torr for the hydrogen pressure and $P_{hydrogen}/P_{butadiene} = 10$)

Sample	Pd_5Pt_{95}	Pd_5Ni_{95}
Pd at.% at surface (from LEIS)	54	50
Catalytic activity (mol cm^{-2} s^{-1})	0.8×10^{15}	8×10^{15}
Selectivity into butenes (at 50% conversion)	93%	100%

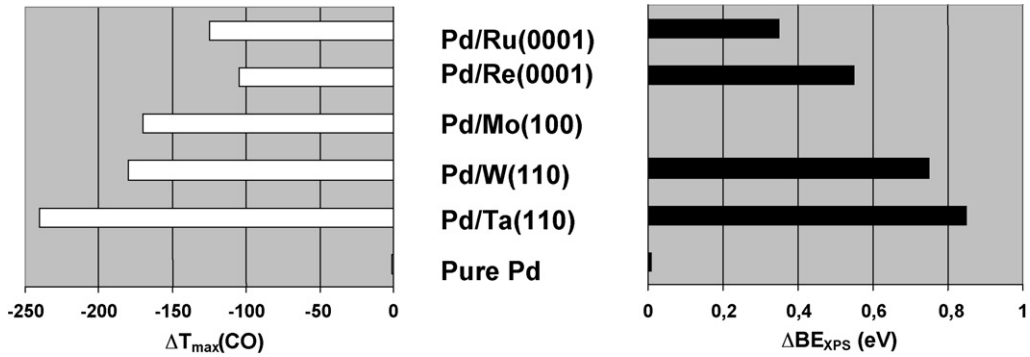

Fig. 12. Correlation between the shift in CO TDS maximum temperature (ΔT_{max}) and the shift of the $Pd_{3d5/2}$ core level energy (ΔBE) for Pd deposits on Ta, W, Mo, Re and Ru single-crystals; values are referred to the corresponding values for pure Pd [29].

Table 3
Surface structure, concentration of the outer layer and catalytic activity for the reaction butadiene → butenes (at 300 K, 10 torr for the hydrogen pressure and $P_{hydrogen}/P_{butadiene}$ = 10) of Pd(1 1 0), Pd_8Ni_{92}(1 1 0), 1 and 4 monolayers (ML) of Pd deposited on Ni(1 1 0) [15–17,31,32]

	Pd(1 1 0)	Pd_8Ni_{92}(1 1 0)	~1 ML Pd/Ni(1 1 0)	4 ML Pd/Ni(1 1 0)
Surface structure	(1 × 1)	(5 × 1)	–	(11 × 2)
Surface composition (Pd at.%)	100	81	70	100
Catalytic activity (mol cm^{-2} s^{-1})	2.14	38	23	74

atoms. Indeed, it is known that electronic effects are largely damped beyond 2–3 atomic distances. In that sense, the behaviour of 4 ML Pd deposits on Ni(1 1 0) is very striking. The Pd film presents then a (11 × 2) reconstruction associated with a large enhancement of its catalytic activity (Table 3) [31,32]. The superstructure comes from periodic edge dislocations initiated by a vacancy in the first Pd layer, which looks like this reported in Fig. 7, but with a larger period. In conclusion, there is a new palladium arrangement with original sites on the surface, which could play an important role in the exceptional catalytic activity.

It would be now important to synthesize core–shell supported Pd–Ni bi-metallic particles to check their catalytic performances. This has been attempted, but no reaction rate amplification was obtained for catalysts having particle size up to about 5–6 nm with Pd coverage of nearby 1–2 ML [33]. One can think that the surface reconstruction observed on extended surfaces cannot occur on small particles because the appearance of a high proportion of unsaturated atoms located at edges and corners; the particle size must be probably larger in order to expose surfaces that are long enough to develop surface reconstruction.

3.3. Specific activities of open surfaces, steps and kinks

Hydrogenation reactions on transition metals are generally considered as independent of the particle size, and consequently of the surface structure, while some differences have been observed as discussed previously. But, issued from surface science data, it is now stated that reactions implying dissociation of molecules depend strongly on the surface structure.

We will consider reactions which imply the dissociation of very stable molecules, like N_2 and CH_4, and hydrogenolysis of some saturated hydrocarbons as examples.

The rate-determining step in iron-catalysed ammonia synthesis is the dissociative adsorption of nitrogen. Using UHV techniques, Ertl reported initial rates for nitrogen adsorption at 550 K to be in the ratio 60:3:1 for Fe(1 1 1), Fe(1 0 0) and Fe(1 1 0), respectively [34]. Somorjaï and co-workers [35] obtained an activity ratio of 418:25:1 for the rate of ammonia formation on iron (1 1 1), (1 0 0) and (1 1 0) samples at 798 K and high pressure (20 atm) of a stoichiometric mixture of hydrogen and nitrogen [35]. Actually, the reactivity for N_2 dissociation is largely higher for the Fe surface exhibiting atoms having the smaller coordination number in its outer layer, that is to say 7 for (1 1 1) of a bcc crystal like Fe, while it is 8 for (1 0 0) and 9 for (1 1 0) surfaces, respectively.

Ruthenium is also now known to be an efficient catalyst for ammonia synthesis. Chorkendorff and co-workers used an elegant way to assert the specific reactivity of steps present on a vicinal face of Ru(0 0 0 1) [36]. Indeed, it is possible to block selectively the step defects on Ru(0 0 0 1), by dosing low content of S, Ag or Au. These elements cause a strong and preferential poisoning at step sites since they bond more strongly on these defect sites than on the close-packed (0 0 0 1) face. This is illustrated in Fig. 13. STM images clearly indicate that Au adsorbs preferentially at step sites [37]. The effect of adding a few percent of a monolayer of Au to the Ru(0 0 0 1) surface is merely to remove the small feature observed at 580 K in TPD spectra following exposure to CO at RT, and associated to CO adsorbed at step sites, showing the preferential blocking of these sites (Fig. 13, right part) [36]. Fig. 14 clearly shows that minority sites like steps are completely dominating the dissociation of nitrogen [36].

Such a conclusion remains valid for other reactions implying the dissociation of highly stable molecules (like CH_4) on metals (like Ni) [38].

The high reactivity of low coordination surface sites present on low-index faces was also clearly evidenced for other reactions implying bond-breaking, such as hydrogenolysis of light hydrocarbons.

As reported in Table 4, activity for light hydrocarbon hydrogenolysis on the kinked [7(1 1 1) × (1 1 0)] Ni surface (see Fig. 2) is 5–10 times higher than on the stepped [7(1 1 1) × (1 0 0)] one (see Fig. 2). Moreover, the close-packed Ni(1 1 1) face does not show significant activity [39].

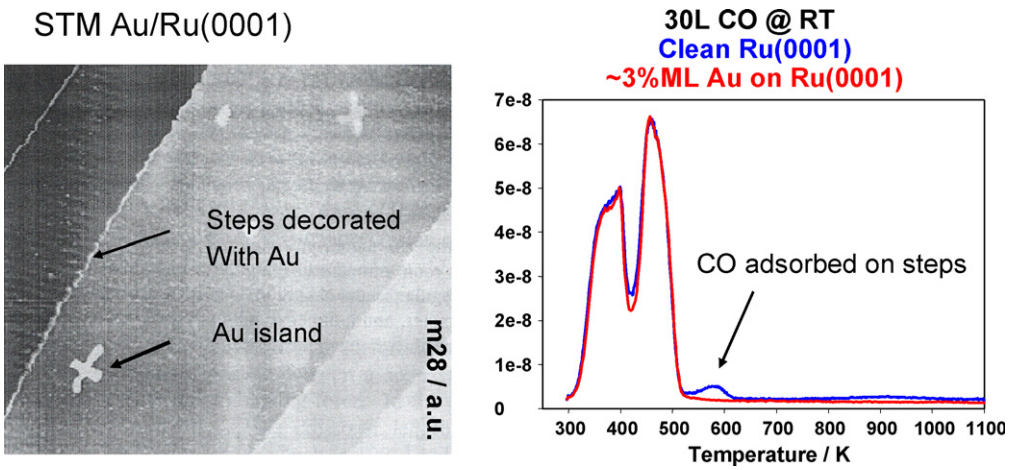

Fig. 13. Left part: STM image (0.7 μm × 0.6 μm) illustrating the preferential decoration of steps on Ru(0 0 0 1) with Au (0.03 ML Au dosed at RT) [37]. Right part: TPD following exposure to 30L CO at RT, before (blue line) and after (red line) adding a few percent of Au to a Ru(0 0 0 1) vicinal surface [36].

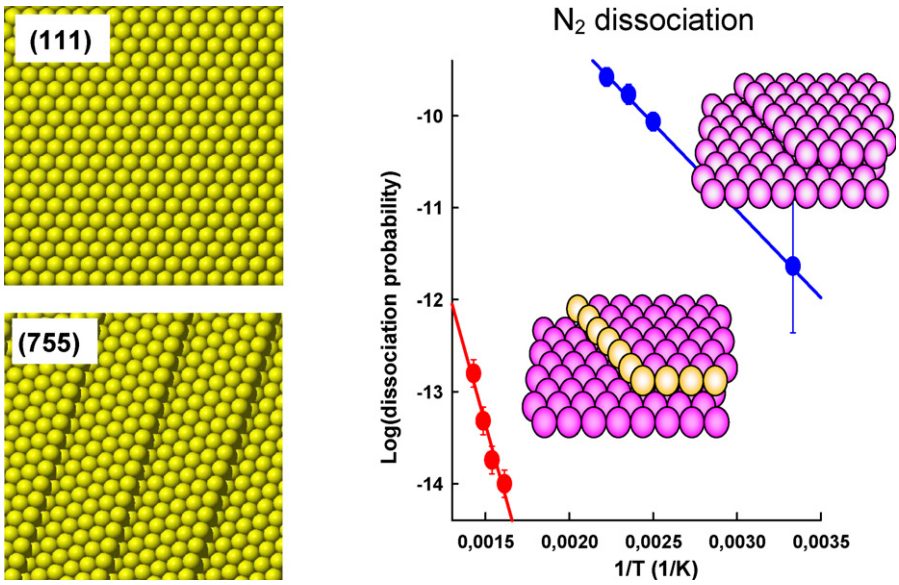

Fig. 14. Illustration of the huge difference in reactivity for N_2 dissociation at the step sites and on the Ru(0 0 0 1) surface (with steps poisoned by Au) [Ib Chorkendorff, personal communication].

For cyclo-pentane, the rate increases following the sequence: (1 1 1) < (1 0 0) < (1 1 0) (Table 4), i.e. it increases when the atomic density at surface (and then the coordination number of surface atoms) is decreased. Taking into account only the atoms on steps and kinks for vicinal surfaces, i.e. assuming a zero activity for (1 1 1) oriented terraces, one sees that the atoms in position of kinks, which have the lowest coordination number ($Z = 6$), are about 10 times more active than those in position of steps ($Z = 7$). Striking is the fact that the surface atoms present on the Ni(1 1 0) face ($Z = 7$) show near the same activity than the atoms located at steps which have the same number of nearest neighbours ($Z = 7$).

Moreover, the different geometry of surface sites may influence not only the activity but also the selectivity, via possible change of mechanism, for a given reaction. The structure sensitivity of alkane skeletal rearrangement reactions has been for example demonstrated on platinum as regards to isomers products, with the use of labelled (C_{13}) hydrocarbons and appropriate tools for localising the various carbons in the reactants and in the reaction products [40].

In conclusion, surface science studies on mono-crystalline vicinal surfaces of transition metals have clearly demonstrated that surface atoms having the less number of nearest neighbours are largely more active for reactions implying bond-breaking.

4. In situ measurements: a challenge for today and further works

For many years surface science experiments devoted to surface characterisation in the field of model catalysis on transition metals and noble metals have been nearly exclusively performed under low pressure conditions. These studies have elucidated many elementary steps of catalytic reactions by the use of single-crystals. Moreover, as discussed previously, many have been also done to bridge the "materials gap" in catalysis with using model supported nano-particles which simulate the behaviour of real catalysts.

Much has now to be done to characterise both the surface structure and the nature of ad-species in working conditions, i.e. under pressure of reactants. In addition, it is important to follow the kinetics of reactions at the same time. This has been attempted recently in some laboratories in the world, and needs the development of specific tools able to look at the interface between a reactive mixture and a working surface of model catalysts, in dedicated reactors.

4.1. Surface structure

Scanning tunnelling microscopy is capable of atomic level measurements while operating over wide pressure range. This makes STM suited for nanoscale in situ studies. The work of Hendriksen and Frenken on CO oxidation on Pt(1 1 0) [41] can be regarded as a sticking example. Insertion of a STM inside a flow reactor allows to demonstrate that, switching from a CO-rich to an O_2-rich flow, one can reversibly oxidize and reduce the platinum surface; this has a dramatic effect on the CO oxidation rate. The presence of the gas phase at high pressure can stabilize surface structures which are not present at low pressure, such as platinum surface oxides, which play an important role in real catalysis.

Measurements at elevated pressure can be also helpful to study the influence of chemisorbed gases having a very low adsorption energy on the structure of metal surfaces. This is for example the case for CO on gold, a metal now considered as the best catalyst for preferential oxidation of CO in presence of hydrogen (PrOx) at low temperature, an important reaction for CO elimination in H_2 for its use in fuel cells. CO does not chemisorb on Au(1 1 0) under low pressure condition at room temperature, or above. But, adsorption is effective under many torr for the CO pressure [42]. In situ STM

Table 4
Compared activities per surface atom (a.u.) for low- and high-index faces of Ni for cyclo-pentane and *n*-butane hydrogenolysis (at 20 torr, H_2/HC = 10) [39]

Reaction/Sample	(1 1 1)	(1 0 0)	(1 1 0)	Stepped [7(1 1 1) × (1 0 0)]	Kinked [7(1 1 1) × (1 1 0)]
Cyclo-pentane (450 °C)	Very low	3100	7300	5300	64000
n-Butane (350 °C)				500	3400

Only the atoms located on steps and kinks are taken into account for vicinal surfaces.

measurements demonstrate that the (1 × 2) missing row reconstruction of this gold surface is then lifted [42]. The specific sites present on the reconstructed Au(1 1 0), which could be a priori regarded as reactive sites, are actually not present in presence of CO adsorbed species.

STM has also been successfully applied to study the evolution of working surfaces of model catalysts constituted by well-defined supported nano-particles, by making a cluster-by-cluster comparison of the morphologic evolution of Au nano-particles during CO oxidation [43,5].

Grazing incidence surface X-ray diffraction (with using synchrotron radiation facilities) offers an alternative and convenient tool for studying surface structure evolution of single-crystal surfaces in reaction condition. For example, it has been shown that the surface structure with $(N \times 1)$ reconstruction observed on the Pd_8Ni_{92}(1 1 0) alloy surface (Fig. 7) is still present during butadiene hydrogenation at 300 K at elevated pressure [17]. It can be therefore stated that the very high reactivity of this sample for this reaction can be related to the structural changes observed.

4.2. Ad-species

Optical vibrational spectroscopies are very appropriate tools for characterisation of surface ad-species at elevated pressure, especially sum frequency generation and polarisation-modulation infrared reflection absorption spectroscopy, or reflection absorption infrared spectroscopy (RAIRS) using *p* and *s* polarised light. Their principles are illustrated in Fig. 15.

In SFG, two laser beams, working in the picosecond regime and temporally synchronised, impact the same area of the analysed sample. One beam is at a fixed energy (visible light) whereas the second beam (in the infrared region) is scanned. In case of a vibrational resonance with an adsorbate vibration, a sum frequency signal is generated: its energy is the sum of the energy of the impacting visible light and the energy of the considered vibration. To be SFG active a vibration must be simultaneously IR and Raman active; thus, a SFG signal is only created at the gas-sample interface and not in the isotropic gas phase, making the technique surface specific. By plotting the SFG signal intensity versus the wavenumber, one obtains a vibrational spectrum.

One of the first experiment with using SFG in surface science devoted to catalysis concerns the mechanism for the hydrogenation of ethylene performed at atmospheric pressure on Pt(1 1 1) by Somorjaï and co-workers. Results are summarized in reference [45]. One can identify the presence of a partially dehydrogenated species, ethylidyne, besides di-σ and π bonded ethylene at surface (Fig. 16). Their relative amount on the surface depends on reaction conditions; they can be correlated with the macroscopic turn over rate measured simultaneously. In fact, ethylidyne species can be considered as "spectators" during hydrogenation. Moreover, the relative amount of active di-σ and π bonded species vary together with the reaction rate, and it is concluded that π bonded ethylene is the most reactive surface species.

This technique has been also successfully applied to other reactions like cyclohexene hydrogenation/dehydrogenation on Pt(1 0 0) and Pt(1 1 1), reactions implying CO and NO on various single-crystal surfaces, and so one [46].

Fig. 17 illustrates the possible use of grazing incidence polarised RAIRS, for CO adsorbed at elevated pressure on Au(1 1 0) [42]. To get such spectra it is necessary to make measurements with *p* and *s* polarised lights. Indeed, with *p* polarised light (parallel to the plane of incidence and perpendicular to the surface plane) it couples with infrared modes characteristic of both the gas phase and of the surface species, while for *s* polarised light (perpendicular to the plane of incidence and then parallel to the surface plane) the signal comes only from contribution of the gas phase. Indeed, as described by the metal selection rules the effective surface sensitivity of *s* polarised light on a metal surface is basically zero. The IR normalized signal (Fig. 17) is then obtained from a combination of I_p and I_s single beam spectra following $[I_p - I_s]/$

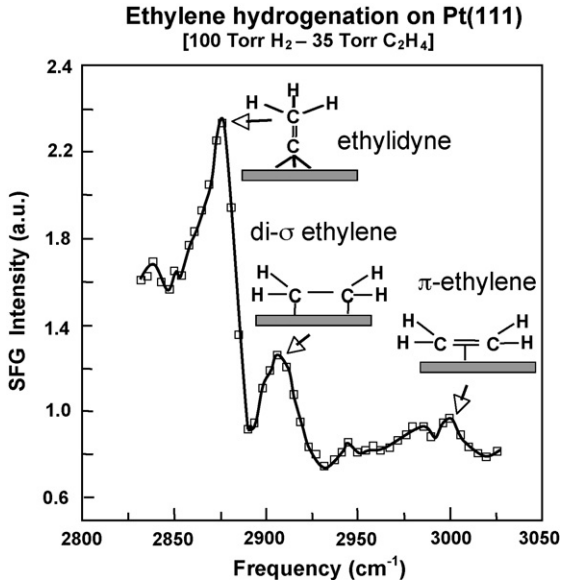

Fig. 16. SFG spectrum of the Pt(1 1 1) surface during ethylene hydrogenation (at 295 K, with 100 torr of H_2, 35 torr of C_2H_4 and 615 torr of He) [45].

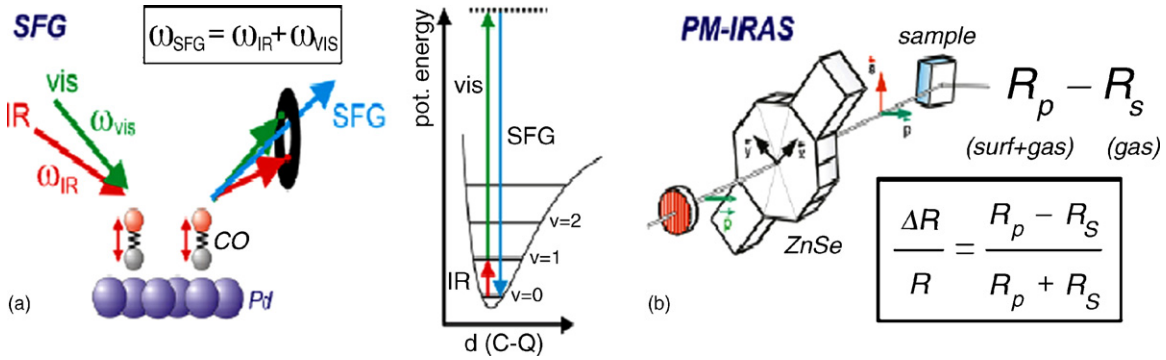

Fig. 15. Schematic representation of (a) sum frequency generation (SFG) and (b) polarisation-modulation infrared reflection absorption spectroscopy (PM-IRRAS) [from ref. [44]].

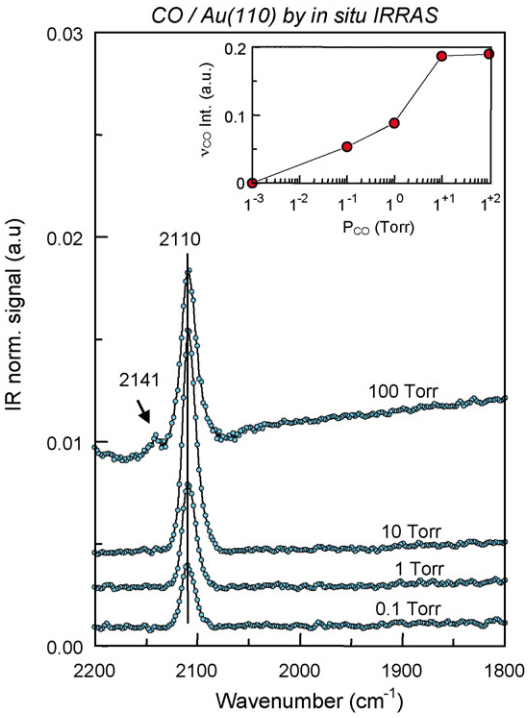

Fig. 17. Polarised RAIRS spectra for CO on Au(1 1 0) under different CO pressures at 300 K [from ref. [42]].

$[I_p + I_s]$. Such a procedure eliminates the gas phase contribution, which is isotropic and insensitive to polarisation effects, and the result is characteristic of only surface adsorbed species.

Better is the use of PM-IRRAS which allows to measure the contribution of surface species and of the gas phase in one step. In fact, polarisation-modulation is performed by a photoelastic modulator (ZnSe) and *p*- and *s*-spectra are acquired simultaneously. The *p*–*s* spectrum characterises then the vibrational characteristics of surface species, and the *s* contribution correspond to the gas phase. As in RAIRS, it is thus possible to measure simultaneously the evolution of reacting mixtures, i.e. the kinetics of reactions, and the nature of ad-species.

In the paper of Rupprechter [44] it is shown that both SFG and PM-IRRAS vibrational techniques can be successfully used to study not only metallic single-crystal surfaces but also model supported nano-particles.

High pressure (some torr) X-ray photoelectron spectroscopy offers now new possibilities to measure the surface composition and study the electronic properties of both the surface itself and the adsorbates [47,48]. It needs a special design of the zone around the sample, allowing it to be kept in a small pressure cell impacted by the X-ray beam, with a small aperture followed by a sophisticated differentially pumped electrostatic lens system able to focus most of the emitted photoelectrons in the energy analyser. Synchrotron radiation facilities are well suited to work in this field, due to the high photon flux available, to the high energy resolution of X-rays and to the variable energy of X-rays, mainly in the low energy range for surface science studies.

In conclusion, observing model catalysts in operating environment offers now opportunities and poses significant new challenges for scientists in the field of catalysis.

5. Conclusions

In conclusion, surface science studies on model catalysts give basic data for reaction understanding and modelling. The Nobel price in chemistry 2007, awarded to Gerhard Ertl for his fundamental works on surface chemistry using model surfaces, attests for the importance of surface science studies for catalytic purposes.

Experimentalists in the field of surface science can provide basic parameters for theoretical works, which can now be applied to rather complex systems using DFT calculations. A strong relation between experimental approaches and theoretical works is therefore needed.

Today nanosciences permit to bridge the so-called ‘materials gap’, by turning out from single-crystal model surfaces to monodispersed nano-particles having a well-defined shape.

In the meantime, works on catalysis at the atomic scale proposes new active/selective sites, and it is now a challenge to design new industrial catalysts on the basis of these fundamental works.

Surface science future outlook has to evolve so that the instrumentation for surface analysis could be used not only in vacuum but also at high pressure, i.e. under realistic conditions where the catalytic processes operate, in order to bridge the “pressure gap”, and also able to work at high temperatures.

Acknowledgements

The author wishes to thank the organisers of the 5th international Paul Sabatier conference on catalysis: “catalysis contribution to key societal challenges”, for giving the opportunity to present this paper to the conference.

Many thanks to Gabor Somorjaï, Hans-Joachim Freund, Ib Chorkendorff and Conrad Becker for providing me viewgraphs and pictures.

References

[1] J.M. MacLaren, B. Pendry, P.J. Rous, D.K. Sadin, G.A. Somorjaï, M.A. Van Hove, D.D. Wedensky (Eds.), Surface Crystallographic Information Service, a handbook of surface, structures, D. Reidel publishing company, Dordrecht/Boston/Lancaster/Tokyo, 1987.
[2] Y. Gauthier, R. Baudoing, Y. Joly, C. Gaubert, J. Rundgren, J. Phys. C: Solid State Phys. 17 (1984) 4547.
[3] B. Lang, R.W. Joyner, G.A. Somorjaï, Surface Sci. 30 (1972) 440.
[4] C.R. Henry, Surface Sci. Reports 31 (1998) 231.
[5] D.W. Goodman, J. Catal. 216 (2003) 213.
[6] H.J. Freund, J. Libuda, M. Baumer, T. Risse, A. Carlsson, Chem. Record 3 (2003) 181.
[7] C. Duriez, C. Chapon, C.R. Henry, C.M. Rickard, Surface Sci. 230 (1990) 123.
[8] M. Schmid, M. Shishkin, G. Kresse, E. Napetschnig, P. Varga, M. Kulawik, N. Nilius, H.-P. Rust, H.J. Freund, Phys. Rev. Lett. 97 (2006) 046101.
[9] G. Hamm, C. Barth, C. Becker, K. Wandelt, C.R. Henry, Phys. Rev. Lett. 97 (2006) 126106.
[10] S. Degen, C. Becker, K. Wandelt, Faraday Discuss. 125 (2004) 343.
[11] D.P. Woodruff (Ed.), The Chemical Physic of Solid, Surfaces, Surface Alloys, Alloy Surfaces, vol. 10, Elsevier, Amsterdam, 2002.
[12] P.W. Wynblatt, R.C. Ku, Surface Sci. 65 (1974) 511.
[13] J.L. Rousset, J.C. Bertolini, P. Miegge, Phys. Rev. B 53 (1996) 4947, References therein.
[14] J.C. Bertolini, Y. Jugnet, The chemical physic of solid surfaces, in: D.P. Woodruff (Ed.), Surface Alloys and Alloy Surfaces, vol. 10, Elsevier, Amsterdam, 2002, , pp. 404–437Cahpter 11.
[15] A.C. Michel, L. Lianos, P. Delichère, N.S. Prakash, J. Massardier, Y. Jugnet, J.C. Bertolini, Surface Sci. 416 (1998) 288.
[16] M. Abel, Y. Robach, J.C. Bertolini, L. Porte, Surface Sci. 454–456 (2000) 1.
[17] M.C. Saint-Lager, Y. Jugnet, P. Dolle, L. Piccolo, R. Baudoing-Savois, J.C. Bertolini, A. Bailly, O. Robach, C. Walker, S. Ferrer, Surface Sci. 587 (2005) 229.
[18] G. Hamm, C. Becker, C.R. Henry, Nanotechnology 17 (2006) 1943.
[19] J.L. Rousset, A.M. Cadrot, L. Lianos, A.J. Renouprez, Eur. Phys. J. D; Atomic Mol. Opt. Phys. 9 (1999) 425.
[20] J.L. Rousset, F.J. Cadete Santos Aires, F. Bornette, M. Cattenot, M. Pellarin, L. Stievano, A.J. Renouprez, Appl. Surf. Sci. 164 (2000) 163.
[21] J.L. Rousset, A.J. Renouprez, A.M. Cadrot, Phys. Rev. B; Condensed Matter Mater. Phys. 58 (1998) 2150.
[22] T. Ouchaib, J. Massardier, A.J. Renouprez, J. Catal. 19 (1989) 517.
[23] J.C. Bertolini, A. Cassuto, Y. Jugnet, J. Massardier, B. Tardy, G. Tourillon, Surface Sci. 349 (1996) 88.
[24] P. Sautet, J.F. Paul, Catal. Lett. 9 (1991) 245.

[25] G. Tourillon, A. Cassuto, Y. Jugnet, J. Massardier, J.C. Bertolini, Chem. Soc. Faraday Trans. 92 (1996) 4835.
[26] J. Silvestre-Albero, G. Rupprechter, H.J. Freund, Chem. Commun. (2006) 80.
[27] H.J. Freund, Catal. today 100 (2005) 3.
[28] J. Silvestre-Albero, G. Rupprechter, H.J. Freund, J. Catal. 230 (2006) 58.
[29] J.A. Rodriguez, The chemical physic of solid surfaces, in: D.P. Woodruff (Ed.), Surface Alloys and Alloy Surfaces, vol. 10, Elsevier, Amsterdam, 2002 , pp. 438–465 (Chapter 12), References herein.
[30] R.W. Judd, A. Reichelt, R.M. Lambert, Surface Sci. 198 (1988) 26.
[31] P. Hermann, J.M. Guigner, B. Tardy, Y. Jugnet, D. Simon, J.C. Bertolini, J. Catal. 163 (1996) 169.
[32] J.S. Filhol, M.C. Saint-Lager, M. De Santis, P. Dolle, D. Simon, R. Baudoing-Savois, J.C. Bertolini, P. Sautet, Phys. Rev. Lett. 89 (2002) 146106.
[33] R. Massard, D. Uzio, C. Thomazeau, C. Pichon, J.L. Rousset, J.C. Bertolini, J. Catal. 245 (2007) 133.
[34] G. Ertl, Catal. Rev. Sci. Eng. 21 (1980) 201.
[35] N.P. Spencer, R.C. Schoonmaker, G.A. Somorjaï, J. Catal. 74 (1982) 129.
[36] R.C. Egeberf, H. Larsen, I. Chorkendorff, Phys. Chem. Chem. Phys. 3 (2001) 2007.
[37] R.Q. Hwang, J. Schröder, C. Gunther, R.J. Behm, Phys. Rev. Lett. 67 (1991) 3279.
[38] F. Abid-Pedersen, O. Lytken, J. Fagbek, G. Nielsen, I. Chorkendorff, J.K. Norskov, Surface Sci. 590 (2005) 127.
[39] J. Massardier, unpublished results.
[40] A. Dauscher, F. Garin, G. Maire, J. Catal. 105 (1987) 233.
[41] B.L.M. Hendriksen, J.W.M. Frenken, Phys. Rev. Lett. 89 (2002) 046101.
[42] Y. Jugnet, F.J. Cadete Santos Aires, C. Deranlot, L. Piccolo, J.C. Bertolini, Surface Sci. Lett. 521 (2002) L639.
[43] A. Kolmakov, D.W. Goodman, Chem. Record 2 (2002) 446.
[44] G. Rupprechter, Catal. Today 126 (2007) 3.
[45] P.S. Cremer, X. Su, Y.R. Shen, G.A. Somorjaï, J. Am. Chem. Soc. 118 (1996) 2942.
[46] G.A. Somorjai, CATTECH 3 (1999) 84.
[47] D. Trschner, A. Pestryakov, E. Kleimenov, M. Hävecker, H. Bluhm, H. Sauer, A. Knop-Gericke, R. Schlögl, J. Catal. 230 (2005) 186, J. Catalysis 230 (2005) 195.
[48] H. Bluhm, K. Andersson, T. Araki, K. Benzerara, G.E. Brown, J.J. Dynes, S. Ghosal, M.K. Gilles, J.C. H-Ch Hansen, A.P. Hemminger, G. Hitchcock, G. Ketteler, A.L.D. Kilcoyne, A.E. Kneedler, R. Lawrence, J.G.G. Leppard, J. Majzlam, B.S. Mun, S.C.B. Myneni, A. Nilsson, H. Ogasawara, D.F. Ogletree, K. Pecher, M. Salmeron, D.K. Shuh, B. Tonner, T. Tyliszczak, T. Warwick, T.H. Yoon, J. Electron Spectrosc. Related Phenomena 150 (2006) 86.